
CHICAGO JOURNALS

The Balloon Experimental Twin Telescope for Infrared Interferometry (BETTII): An Experiment for High Angular Resolution in the Far-Infrared
Author(s): S. A. Rinehart, M. Rizzo, D. J. Benford, D. J. Fixsen, T. J. Veach, A. Dhabal, D. T. Leisawitz, L. G. Mundy, R. F. Silverberg, R. K. Barry, J. G. Staguhn, R. Barclay, J. E. Mentzell, M. Griffin, P. A. R. Ade, E. Pascale, G. Klemencic, G. Savini, and R. Juanola-Parramon
Source: *Publications of the Astronomical Society of the Pacific*, Vol. 126, No. 941 (July 2014), pp. 660-673
Published by: The University of Chicago Press on behalf of the Astronomical Society of the Pacific
Stable URL: http://www.jstor.org/stable/10.1086/677402
Accessed: 31/01/2015 17:02

Your use of the JSTOR archive indicates your acceptance of the Terms & Conditions of Use, available at http://www.jstor.org/page/info/about/policies/terms.jsp

JSTOR is a not-for-profit service that helps scholars, researchers, and students discover, use, and build upon a wide range of content in a trusted digital archive. We use information technology and tools to increase productivity and facilitate new forms of scholarship. For more information about JSTOR, please contact support@jstor.org.

The University of Chicago Press and *Astronomical Society of the Pacific* are collaborating with JSTOR to digitize, preserve and extend access to *Publications of the Astronomical Society of the Pacific.*

http://www.jstor.org

This content downloaded from 128.154.225.202 on Sat, 31 Jan 2015 17:02:50 PM
All use subject to JSTOR Terms and Conditions

PUBLICATIONS OF THE ASTRONOMICAL SOCIETY OF THE PACIFIC, **126**:660–673, 2014 July
© 2014. The Astronomical Society of the Pacific. All rights reserved. Printed in U.S.A.

The Balloon Experimental Twin Telescope for Infrared Interferometry (BETTII): An Experiment for High Angular Resolution in the Far-Infrared

S. A. RINEHART,[1,2] M. RIZZO,[3,2] D. J. BENFORD,[2] D. J. FIXSEN,[3,2] T. J. VEACH,[4,2] A. DHABAL,[3,2] D. T. LEISAWITZ,[2] L. G. MUNDY,[3] R. F. SILVERBERG,[5,2] R. K. BARRY,[2] J. G. STAGUHN,[6,2] R. BARCLAY,[2] J. E. MENTZELL,[2] M. GRIFFIN,[7] P. A. R. ADE,[7] E. PASCALE,[7] G. KLEMENCIC,[7] G. SAVINI,[8] AND R. JUANOLA-PARRAMON[8]

Received 2014 April 18; accepted 2014 May 31; published 2014 July 10

ABSTRACT. The Balloon Experimental Twin Telescope for Infrared Interferometry (BETTII) is a new balloon-borne far-infrared interferometer, being designed to provide spatially-resolved spectroscopy in the far infrared (30–90 μm). The combination of an 8-meter baseline with a double-Fourier Michelson interferometer allows the identification and separation of closely-spaced astronomical sources, while also providing a low-resolution spectrum for each source. In this wavelength range, BETTII will provide subarcsecond angular resolution, a capability unmatched by other far-infrared facilities. This paper provides an overview of the entire design of the BETTII experiment, with a short discussion of the predicted performance on flight.

Online material: color figures

1. INTRODUCTION

Far-infrared (FIR) astronomy has made many important contributions to astrophysics, but these observations have been and continue to be limited by the angular resolution achieved with single aperture telescopes (Acke et al. 2012; Kamp et al. 2013). While collecting area is clearly important for observing faint sources, in the far-infrared photons are plentiful, and deep surveys are limited not by the collecting area but by source confusion due to the inherently low angular resolution (Rigby et al. 2011; Nguyen et al. 2010). Interferometry provides significant improvements in angular resolution without increasing total aperture size, decoupling sensitivity from angular resolution. Sensitivity is governed by the size of individual collector mirrors, while angular resolution is governed by the maximum baseline of the interferometer.

The potential of interferometers in the far-infrared has been recognized for some years, and led to a Vision Mission study of the Submillimeter Probe of the Evolution of Cosmic Structure (SPECS; Harwit et al. 2006) and an Origins Probe study of the Space Infrared Interferometric Telescope (SPIRIT; Leisawitz et al. 2007). The first of these was envisioned as an ambitious mission for the future, with a 1-kilometer maximum baseline and two 4-meter diameter collector telescopes, connected with tethers. SPIRIT was studied as a structurally-connected interferometer with a maximum baseline of ~36 meters and individual collecting telescopes with ~1 meter apertures. In the far-infrared, the system-level requirements (e.g., pointing, metrology) for a mission such as SPIRIT are feasible with existing technology, while the instrument itself would require only modest technology development (e.g., improved detectors; Leisawitz et al. 2012).

The Balloon Experimental Twin Telescope for Infrared Interferometry (BETTII) was inspired by these mission concepts, and conceived both as a technical pathfinder for these missions and a scientifically valuable experiment in its own right (Rinehart 2010). BETTII is an eight-meter, fixed-baseline FIR interferometer to fly on a high-altitude balloon. The instrument itself is a double-Fourier Michelson interferometer (Mariotti & Ridgway 1988). Because of the fixed baseline, complex image reconstruction is not the aim of the mission; rather, the goal is to provide spatially-resolved spectroscopy, whereby individual point sources or sources with simple (symmetric) morphologies can be isolated and characterized with low-resolution ($R < 200$) spectra. The uniquely high resolution of BETTII at FIR wavelengths allows the study of the distribution of warm dust associated with the most active regions of star formation in nearby galactic star-forming clusters and in the nuclei of active galaxies.

From a technical perspective, BETTII demonstrates the technical maturity of individual components needed for future space-based interferometers (e.g., mechanisms). More importantly, it provides a clear system-level demonstration of an

[1] Stephen.A.Rinehart@nasa.gov, 301-286-4591.
[2] NASA Goddard Space Flight Center, Mail Code 665, Greenbelt, MD, 20771.
[3] Astronomy Department, University of Maryland, College Park, 20742.
[4] Oak Ridge Associated Universities, NASA Postdoctoral Program Fellow.
[5] Universities Space Research Association.
[6] The Henry A. Rowland Department of Physics and Astronomy, Johns Hopkins University, 3400 N. Charles Street, Baltimore, MD 21218.
[7] School of Physics and Astronomy, Cardiff University, Cardiff, CF24 3AA, UK.
[8] Optical Science Laboratory, Department of Physics and Astronomy, University College London, London WC1E 6BT, UK.

This content downloaded from 128.154.225.202 on Sat, 31 Jan 2015 17:02:50 PM
All use subject to JSTOR Terms and Conditions

interferometer in a space-like environment. In fact, the balloon environment is, in many respects, even more challenging than the space environment. For example, while the atmospheric density is extremely low at these altitudes, winds and localized temperature variations can excite small perturbation motions in the gondola, including pendulation. For an interferometer, this can be very problematic, as such perturbations can lead to significant phase noise and compromise data quality.

In this paper, we present the overall design of the BETTII experiment, discuss the expected performance, and describe the planned first science campaign. This is intended as a broad overview; it is beyond the scope of this paper to provide a high level of detail on individual systems. Details on subsystems will be presented in upcoming papers (Rinehart et al. 2014; Rizzo et al.2014a; Veach et al. 2014; Benford et al. 2014) and in other future publications. BETTII is currently in the fabrication phase, and is on schedule for launch in 2015 fall from Fort Sumner, New Mexico.

2. THE BETTII EXPERIMENT

BETTII is a balloon-borne 8-meter baseline Michelson stellar interferometer utilizing two elliptical siderostats that have beams on the sky corresponding to 50 cm diameter circular apertures (Fig. 1). The cryogenic instrument has two wavelength bands (30–55 and 55–90 μm), providing angular resolution of 0.5" at 40 μm, and spectral resolution of up to R $\sim$ 200. BETTII has an approximate mass of 1,000 kg; on an 11.82 million cubic foot balloon, BETTII should reach an altitude of 120,000 feet. While BETTII can, in principle, obtain scientific data during daylight hours, for the first flight it is desirable to maximize the amount of dark time at float. Assuming a morning launch from Fort Sumner, this will require total flight times of $>$16 hr.

The instrument itself is a "double-Fourier" Michelson interferometer, similar to that envisaged for potential high-performance space-based interferometers (e.g., SPIRIT). The double-Fourier instrument provides two key advantages for BETTII. First, it provides both spatial and spectral information simultaneously. Second, it allows for wide-field interferometry.

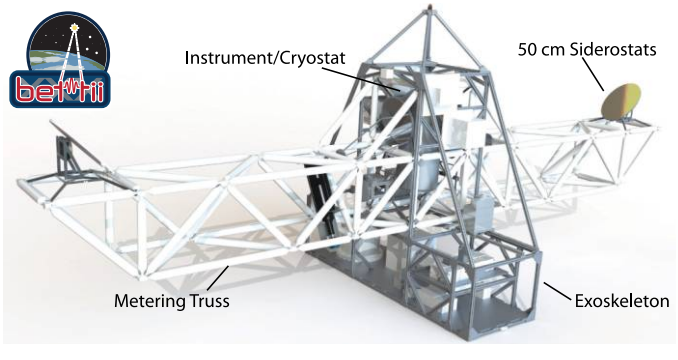

FIG. 1.—The overall design of BETTII is shown here. This paper is divided into three major sections, corresponding to the major elements identified within this figure: the external optics (metering truss), the instrument, and the exoskeleton/control system. See the electronic edition of the *PASP* for a color version of this figure.

A traditional Michelson interferometer uses a single detector; the field of view (the "primary beam") is determined by the size of the individual light collection apertures. By using a detector array, one observes interferograms corresponding to multiple contiguous primary beams simultaneously on different pixels. Spatial information is encoded on the detector as a relative shift in the zero path difference (ZPD) location between the white light fringe packets from different sources. A double-Fourier interferometer, equipped with a modest detector array, can therefore provide simultaneous high spatial resolution and moderate spectral resolution over a wide field of view. This technique has been demonstrated previously (Rinehart et al. 2012), and a much more extensive discussion is provided by Leisawitz et al. (2012).

For the purposes of this paper, we consider BETTII to be coarsely divided into three major subsystems: the warm optical system, the cryostat/instrument, and the control system/exoskeleton. In this paper, we describe some of the top-level requirements on BETTII then present the broad design of the experiment. We also briefly discuss the expected performance of BETTII, and comment upon future work.

2.1. Requirements

In developing the concept for BETTII, the underlying scientific goal was to be able to carry out FIR observations that sample the SED peaks of cool ($\sim$50 K) material at low spectral resolution, but with sufficient angular resolution to differentiate emission from a group of closely-spaced sources that are unresolved by single mirror systems. This objective leads directly to the three top-level requirements on BETTII: it must operate at high altitude (120,000 feet), where high atmospheric transmission makes FIR observations possible; it must be a spatial interferometer to provide high spatial resolution; and it must be a double-Fourier instrument in order to obtain astrophysically interesting spectra from sources across a wide field of view.

These top level requirements, as well as the specific science cases that motivate BETTII, lead to several specific technical requirements on the experiment (Table 1). The majority of these requirements, such as instrument field-of-view, are self-explanatory, but two parameters in particular are worthy of some additional discussion. First, the required pointing stability is 1.5″, over timescales of 10 s. This stability constrains drift of the beam on the sky to under 10% of a detector pixel, on timescales longer than a single delay line scan (2.5 s). This prevents distortion of the fringe pattern due to changes in the relative pointing of the system; such distortion leads to a significant reduction in signal-to-noise ratio (S/N) and to errors in the reconstructed spectrum.

Second, high frequency pointing jitter must be tightly controlled. High frequency jitter in the mechanical system is manifested in the interferometric data directly as phase noise; unmitigated phase noise, in turn, effectively "washes out" the

This content downloaded from 128.154.225.202 on Sat, 31 Jan 2015 17:02:50 PM
All use subject to JSTOR Terms and Conditions

TABLE 1
SCIENTIFIC REQUIREMENTS FOR THE BETTII EXPERIMENTS

Science Requirement	Parameter	Value	Technical Implementation
Coverage of clusters	Field-of View	2 arcmin	Wide field-of-view interferometry; detector arrays
Detection of cores in clusters	Sensitivity	<40 Jy, 5σ, 10 minutes	Siderostat size, cryogenic instrument
Detection of broad spectral features	Spectral Resolution	$R \sim 20$	Delay line stroke length
Resolution of cores	Spatial Resolution	1 arcsec	8-meter baseline
Map warm dust	Wavelength Range	30–90 μm	BUG detector arrays
Spectral Fidelity	Pointing Stability	1.5"	Star camera, fiber optic gyro
Interferometric Visibility	Pointing Jitter	$0.1''$, <10 Hz	Stiff structure, vibration isolation

interferometric fringes, reducing the S/N of the fringes. The $0.1''$ requirement ensures that jitter-induced instrumental visibility loss is $<5\%$.

2.2. Warm Optical System

The warm optical system (the system located outside of the instrument cryostat) is designed to collect two 50 cm diameter wavefront samples and to provide compressed 2.5 cm diameter, co-phased, commonly rotated beams to the central double Fourier beam-combining instrument. To achieve this purpose, the system includes the metering truss, the siderostats, the telescope assemblies, the k-mirror, and the warm delay line.

The metering truss (Fig. 2) is designed to serve as an optical bench. As such, it must be stiff. In addition, the truss must be well-behaved (i.e., it should not twist or warp) over large temperature changes; on the ground, prior to launch, temperatures can be as high as 35° C. At float, the temperature is expected to be ~ -40°C. In order to achieve the high altitudes desired for high atmospheric transmission, the truss must be lightweight. Finally, to meet requirements of NASA's Columbia Scientific Ballooning Facility, it must survive a 10-g vertical load.

The primary material for the metering truss is carbon fiber; such structures have been shown to be strong, stiff, and light (Ogasaka et al. 2005). The structure itself has reflection symmetry for the two arms of the interferometer. This symmetry ensures that structural changes due to thermal effects are nearly identical for both arms of the interferometer. The individual members of this structure are 3-inch carbon fiber tubes, with a stainless-steel "nose-cone" attached in each end using two-part epoxy. Each tube was tested by placing ~2000 pounds of stress along the length of the tube (twice the maximum load on a tube during a 10-g acceleration), to verify both the carbon fiber tube strength and the epoxy bond strength. Only a single nose-cone bond failed (out of a total of 250), giving a high level of confidence in the individual members of the metering truss. The metering structure consists of individual tubes of three different lengths, and the tubes are connected via stainless steel nodes. Only two different types of nodes are used within the structure. One advantage of the design is the low number of unique part designs; this simplifies replacement of damaged components, simplifies construction, and minimizes the numbers of spare components needed. Finite element analysis shows a first vibration mode for the structure at 24.8 Hz; this has been measured in the laboratory at 24.0 Hz. This mode is symmetric, consisting of vertical "flapping" of the two arms of the structure. The second mode is similar to the first, but antisymmetric, with one arm moving upward while the other moves down. This mode is predicted at 30.6 Hz, and measured in the laboratory at 28.0 Hz. Additional details on the metering truss, as well as both the modeled and measured performance, will be described in an upcoming paper.

One consideration in the design the optical truss is the time required for thermalization of the structure. While, for the first BETTII flight, scientific data acquisition will occur at night, the launch itself will occur during daylight hours. Illumination from the sun can result in thermal gradients within the structure, and hence deformation of the truss. However, this is largely

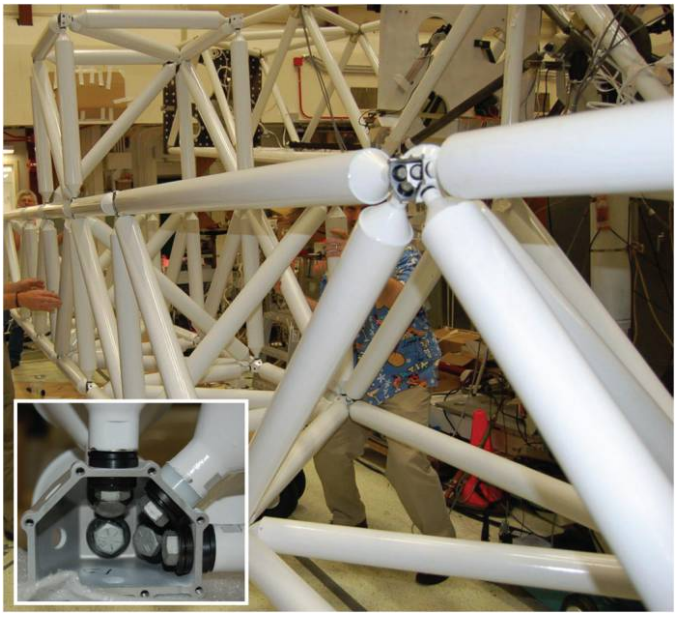

FIG. 2.—The BETTII truss was completed in 2012; the picture here shows the truss immediately after assembly. The inset picture shows additional detail. The individual tubes are connected together via stainless steel nodes. Each of the connections to the node uses a single 3/8″ bolt, with spherical washers to allow flexure of the truss. For longer tubes, polyethylene washers are used in order to compensate for the differential thermal contraction anticipated as the payload ascends to balloon altitude. See the electronic edition of the *PASP* for a color version of this figure.

This content downloaded from 128.154.225.202 on Sat, 31 Jan 2015 17:02:50 PM
All use subject to JSTOR Terms and Conditions

mitigated through the low CTE of the carbon fiber structure; the structure should meet all requirements even during daytime operation. In addition, the truss is coated with a white epoxy paint, in order to minimize heating of the structure. The concern with thermal gradients is also relevant for the telescope structure; this concern drives the desire for BETTII to operate after sunset. The telescope optics and structure are all aluminum, and the $1/e$ thermalization time for these components is 6 minutes; 20 minutes after sunset, the telescope structure should be nearly isothermal.

The metering truss serves a single purpose: to act as a stable 8-meter long optical bench for the warm optics. The external optical design is shown in Figure 3. Light arriving at the interferometer from an astronomical source impinges upon two siderostats mounted at opposite ends of the metering truss; each is attached to a rotation stage which allows elevation pointing. Light reflects off the siderostats and enters the two nominally identical telescope assemblies, which compress the collimated 50 cm input beams by 20:1 down to 2.5 cm collimated output beams. Each of the telescope assemblies consists of four mirrors: a primary mirror, a flat mirror, a secondary, and a tertiary (Fig. 4). This four-mirror design meets the BETTII wavefront requirements (RMS errors of <0.2 μm), and has reasonable alignment requirements (positions to within 75 μm, angles to within 7″), dominated by wavefront requirements in the short wavelength science channel. The structure of the telescope assembly consists of a mounting ring for the primary, a mounting ring for the flat mirror, separate 3-point mounts for the secondary and tertiary, and a connecting "trough". The rings isolate the mirrors, limiting optical distortion transmitted from the sag in the trough. The trough provides both high stiffness and high strength at low mass. The entire assembly, including both the structure and the individual mirrors, is made of aluminum, so that it undergoes homologous contraction over the large temperature change expected from launch-to-float (i.e., the optical prescription is conserved with changes in temperature).

On the ground, the two telescope assemblies can be aligned to within ∼10″; by adjusting flat mirrors in the warm delay line and the K-mirror assemblies, these beams can then be aligned to within ∼2″. On flight, in order to maintain high interferometric fringe visibility, the relative alignment needs to be maintained to within ∼0.5′. This is achieved by using identical, symmetric

FIG. 4.—All components of the telescope assembly, including the mirrors themselves, are aluminum, in order to ensure that the entire structure shrinks homologously through the ground-to-float temperature differential. The inset figure shows a top view of the structure. Both assemblies will be built, aligned, and tested on the bench prior to integration into the metering truss. This structure was designed in collaboration with the Precision Engineering Center at North Carolina State University, and is currently in fabrication.

mounting structures for both telescopes, and having them both mounted to the stable metering truss, which was designed for this purpose.

Following the telescope assemblies, the layouts of the two arms of the interferometer differ. In one arm of the interferometer, the collimated beam travels through a warm delay line (the WDL) consisting of four mirrors, all mounted at 45° angles relative to the incident beam (Fig. 5). Two of these mirrors are mounted on a linear travel stage, allowing changes to the optical path length but without any impact on the alignment of the beam. The warm delay line is used to compensate for variations in the optical path length difference between the two arms of the interferometer. We expect that pendulation will dominate phase variation for BETTII, although lower amplitude vibrations in the structure can also be compensated by the warm delay line,

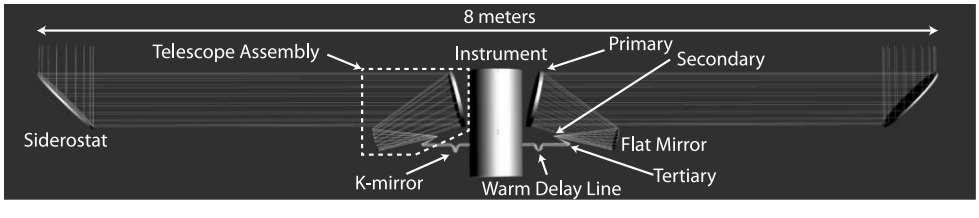

FIG. 3.—The BETTII warm optics system consists of two siderostats which transfer beams on the sky to the telescope assemblies. There are separate telescope assemblies (*inside the dashed-line box on the left*) for each arm; the two are identical in design, and consist of three powered mirrors and a single flat mirror. One arm of the interferometer includes the warm delay line, while the other arm includes a K-mirror assembly.

This content downloaded from 128.154.225.202 on Sat, 31 Jan 2015 17:02:50 PM
All use subject to JSTOR Terms and Conditions

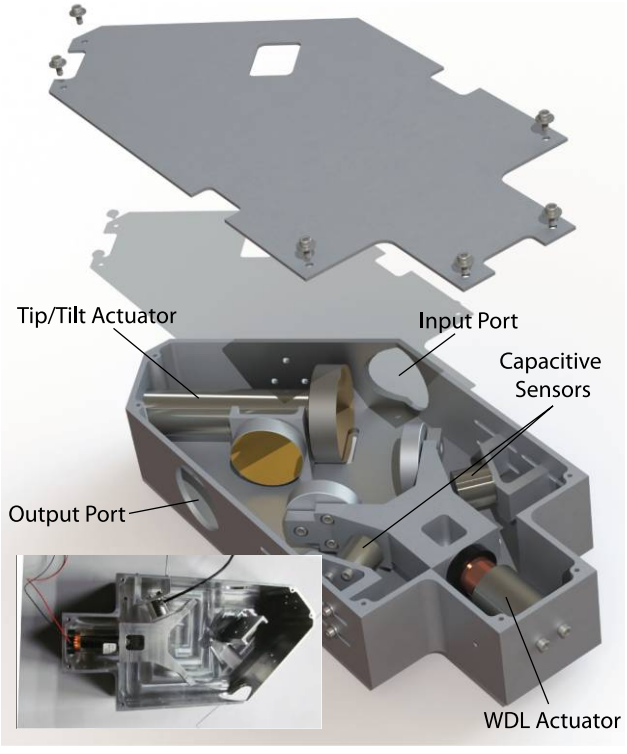

FIG. 5.—The Warm Delay Line (WDL) consists of four flat mirrors, configured such that the input and output beams are coaxial. Two mirrors sit on a linear travel stage, actuated by a single motor. A pair of capacitive sensors provide knowledge of the WDL position, and a single tip/tilt stage is located within the WDL for use in the control system. For scale, the mirror on the tip-tilt stage is 2 inches in diameter. See the electronic edition of the *PASP* for a color version of this figure.

as described in section 2.4, below. Following the warm delay line, the beam continues to the cryostat.

In the other arm of the interferometer, the collimated beam enters a K-mirror assembly (Fig. 6), the purpose of which is to rotate the image to match that of the arm with the warm delay line. The K-mirror consists of three mirrors, arranged such that the axis of the incoming and outgoing beams from the assembly are aligned. The assembly is mounted to a rotation stage, enabling rotation of the field-of-view by up to 360°. The K-mirror assembly is needed for BETTII because the differing orientations of the two siderostats produce opposing field-of-view rotations. Following the K-mirror, the beam continues to the cryostat.

As shown in Figures 5 and 6, both the warm delay line and the K-mirror assembly include a fast tip-tilt stage. These tip/tilt stages respond to signals from the BETTII control system to align the pointing of the two arms of the interferometer, as described in section 2.4. To achieve the scientific goals of the BETTII experiment, all optical elements of the warm optical system must have RMS surface roughness smoother than 0.1 μm, with figure errors of less than 0.1 μm. The external optical system operates at ambient temperature (~240 K at float

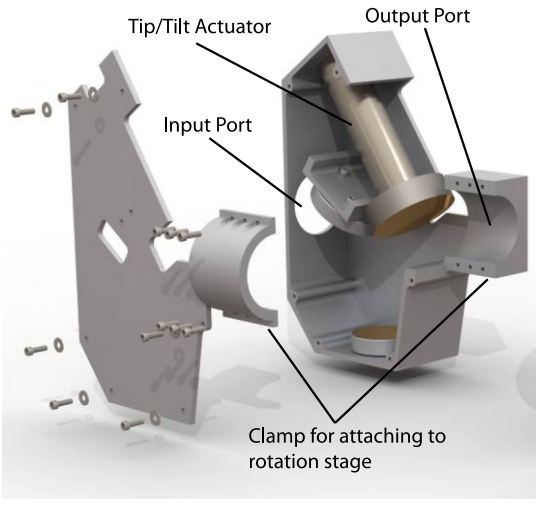

FIG. 6.—The K-mirror is a common design used for beam rotation; it consists of three flat mirrors, arranged so that the input and output beams are coaxial. One of the three mirrors is mounted on a tip/tilt stage for use by the control system. For scale, the mirror not the tip-tilt stage is 2 inches in diameter. See the electronic edition of the *PASP* for a color version of this figure.

altitudes of 120,000 feet). These "warm" optics limit the overall sensitivity of the instrument (see section 3).

2.3. Instrument

The second major BETTII system is the instrument itself. The instrument is defined, in this context, as the cryostat and all components within it, including the cold optics, the cryogenic delay lines, cryogenic systems, and detectors, as well as external components needed for operation of these elements.

The BETTII cryostat was custom designed at NASA Goddard. This approach was driven by several requirements: long (24-hr) hold times were required for operation during a balloon flight; the cold (helium-cooled) volume must be sufficiently large to hold the science instrument, with adequate volume for a Helium-3 refrigerator (to cool the detector arrays to 300 mK); there must also be a cool (nitrogen-cooled) volume for the near-infrared channel. A cutaway view of the cryostat is shown in Figure 7. The cryostat has a 15-liter tank for liquid nitrogen and a 22-liter tank for liquid Helium. Manostats are used to maintain atmospheric pressure within them while the instrument is at float altitude, in order to reduce boil-off of the cryogens, increase cryogenic hold time, and to provide thermal stability. Inside the cryostat, there are two distinct instrument channels: a science (far-infrared) channel, and a tracking (near-infrared) channel.

The cryostat is attached to the metering truss with an assembly constructed of titanium and aluminum. This structure maintains the position of the dewar window relative to the beam from the external optics to within 200 μm even through the large expected temperature change.

This content downloaded from 128.154.225.202 on Sat, 31 Jan 2015 17:02:50 PM
All use subject to JSTOR Terms and Conditions

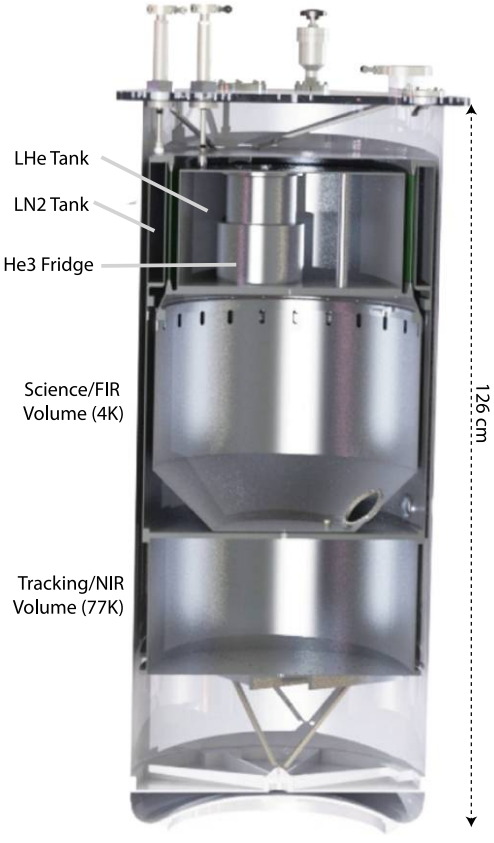

FIG. 7.—The custom cryostat design uses liquid nitrogen and liquid helium to achieve 4K operation. A dual-stage He4/He3 refrigerator cools the detector arrays to 300 mK. See the electronic edition of the *PASP* for a color version of this figure.

The beams from the external optics enter the cryostat through thin (15 μm) polypropylene windows. These windows provide good transmission at both near- and far-infrared wavelengths while also minimizing thermal emission. The windows will deform significantly with a 1 atmosphere pressure difference, but tests have shown that the material reliably holds to several atmospheres of pressure. The first cold optical system element is the near-infrared beamsplitter. The beamsplitter reflects light into the BETTII science channel, transmitting the NIR light into the tracking channel.

2.3.1. The Science Channel

A block diagram of the optics in the FIR channel is shown in Figure 8, and the corresponding physical layout is shown in Figure 9. The FIR beams travel through an optical relay, creating a cold pupil inside the cold volume for use in stray light control. A flat mirror then steers the beam into the cold delay line (described below). Following the cold delay line, another flat mirror steers the beams to the far-infrared beam combiner. This beam combiner, a hot pressed wire mesh beamsplitter, has close to 50/50 transmission/reflection across the entire science

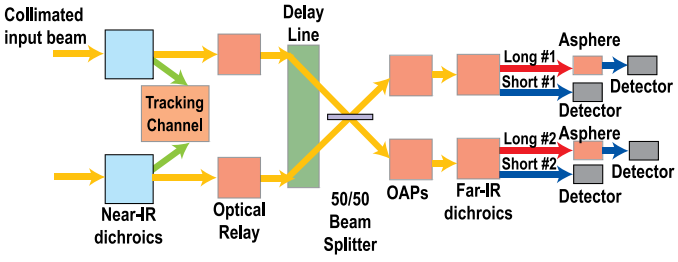

FIG. 8.—The optical layout in the science channel is shown in Fig. 9, but because the cold optical system makes use of all three dimensions to fit within the cryostat, the system is more easily understood with the aid of this block diagram, showing the key optical elements. These include the optical relay, the cold delay line, the beam combiner, the camera optics, and the dichroics. See the electronic edition of the *PASP* for a color version of this figure.

band, 30–90 μm, and will be fully characterized at Cardiff University prior to delivery. Both of the outputs from the beam combiner travel to spherical mirrors which serve as the camera optic for the short wavelength (30–55 μm) channel. The converging beam then impinges upon a FIR dichroic, which splits the FIR light into two bands. There are now four beams within the instrument, beams from both output ports of the beam combiner for each of the two wavelength channels. The short wavelength beams reflect off the dichroic to their detector arrays, while the long wavelength (55–90 μm) beams are transmitted by the dichroic to a final powered mirror, and then to the detector arrays. This final powered mirror is needed to adjust the overall focal length of the long-wavelength channel, and hence the plate scale on the detector arrays.

One of the key components of the instrument is the cold delay line (CDL). The CDL is used to modulate the relative phase between the two arms of the interferometer (Fig. 10). This structural design is based upon Variable Polarization Modulators (VPMs: Chuss et al. 2006, 2012) built at Goddard. The majority of the CDL structure (Fig. 10) is made out of aluminum, with titanium flexures to maintain linearity of travel. At the center of the CDL is the aluminum mirror assembly. This comprises two rooftop mirror pairs built back-to-back. This provides optical delay of four times the physical stroke of the delay line. The CDL is driven by a voice coil and has a physical stroke length of 2.5 mm, providing 10 mm of optical path change. Two capacitive sensors are used to measure the position of the delay line to within a few tens of nanometers.

In scientific operation, the CDL will conduct a single scan every 2.5 s, and successive scans will be co-added for a total observing time on target of 18 minutes. Observing with BETTII will be broken into 18-minute observing blocks; during the first flight, we plan to interleave observing blocks on scientific sources with observing blocks on external calibrators, to ensure that we are obtaining good quality fringes, and to understand and characterize the performance of the system and measure the instrumental visibility loss. Ultimately, however, the system

This content downloaded from 128.154.225.202 on Sat, 31 Jan 2015 17:02:50 PM
All use subject to JSTOR Terms and Conditions

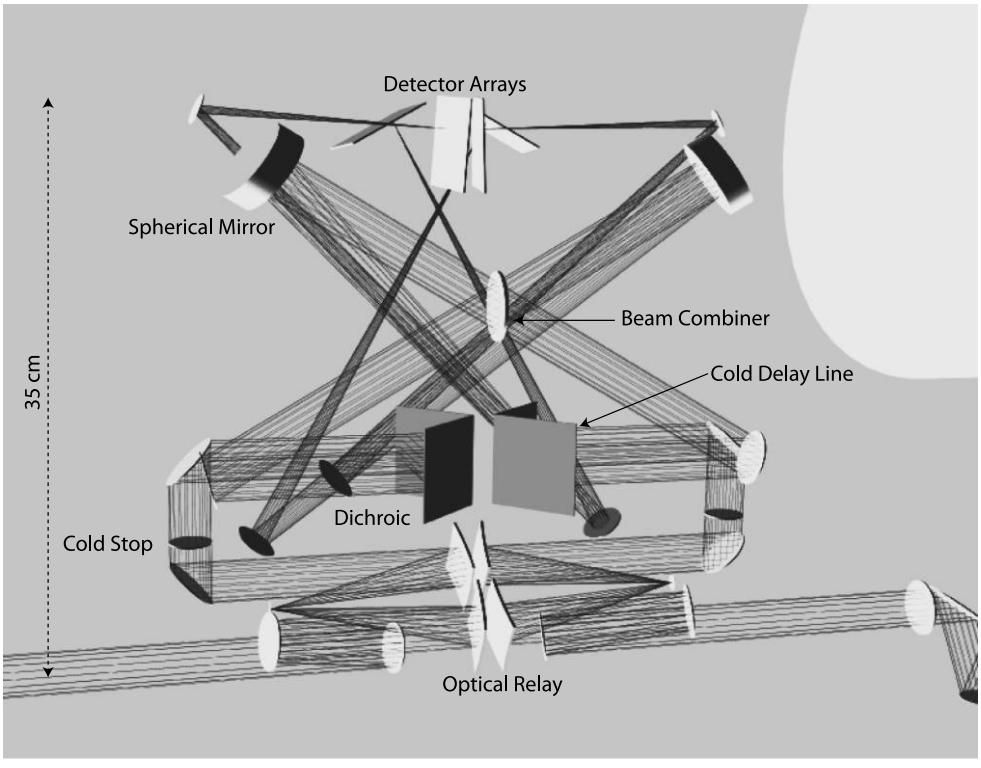

FIG. 9.—The cold optical system folds in three dimensions to fit inside the cryostat. The reflection symmetry of the design simplifies assembly. Major components are labeled here for clarity.

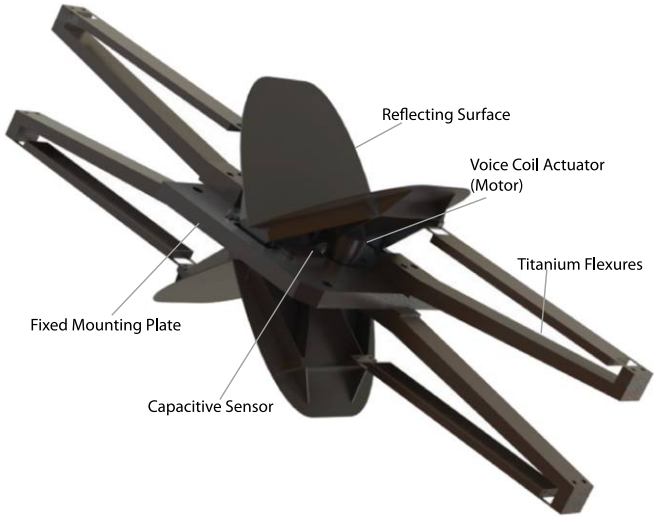

FIG. 10.—The cold delay line consists of a pair of rooftop mirrors mounted back-to-back, attached to a fixed mounting plate via titanium flexures. The mirrors are actually a single unit, and are moved using a voice coil actuator. The flexures allow the mirrors to move linearly along the axis of the incoming beam (s). For scale, the total distance between the ends of the flexures is 10.4 inches. See the electronic edition of the *PASP* for a color version of this figure.

should be sufficiently stable that observations of a single source can continue over multiple observation blocks.

The BETTII instrument is a multichannel bolometric camera. The FIR light efficiently couples to the detectors using resonant absorption. BETTII has four detector arrays, one for each of two bands on each of two output ports of the beam combiner. Each array is a 9×9 close-packed planar array of multiplexed superconducting transition edge sensor (TES) bolometers (Benford et al. 2008) incorporating the Backshort Under Grid (BUG) architecture (Allen et al. 2006). The bolometer arrays are designed as scaled versions of existing bolometer arrays that have been used for ground-based instruments (e.g., GISMO; Staguhn et al. 2006, 2014). By scaling predominantly only leg geometry for the same transition temperature, the BETTII arrays have increased saturation power and faster response times relative to GISMO, both needed by BETTII. As the sensitivity of BETTII is limited by the emission from the ambient temperature optics, the background loads are relatively high; the detectors must be capable of handling up to 200 pW of illuminating power. Fast response time allows for high speed detector readout, which is needed to sample interferometric fringes during the fast delay line scans described above. Table 2 lists all of the relevant parameters of these detectors.

The BETTII bolometers will be read out by an advanced linear SQUID multiplexer with heritage from prior instruments such as GISMO (Staguhn et al. 2008). A key advance is the use of

This content downloaded from 128.154.225.202 on Sat, 31 Jan 2015 17:02:50 PM
All use subject to JSTOR Terms and Conditions

TABLE 2
DETECTOR PARAMETERS

Parameter	Short Band	Long Band
Pixel Pitch	13.3 arcsec/pixel	16.7 arcsec/pixel
Array Size	9×9	9×9
Field-of-View	2.0 arcmin^2	2.5 arcmin^2
Photon NEP	1.38×10^{-15} W Hz$^{-1/2}$	7.4×10^{-16} W Hz$^{-1/2}$
Detector NEP	3.0×10^{-16} W Hz$^{-1/2}$	3.0×10^{-16} W Hz$^{-1/2}$
Readout Speed	400 Hz	400 Hz
Time Constant	1.7 ms	1.7 ms

high-order radiometric coils that reduce the sensitivity to environmental magnetic fields by orders of magnitude compared to early SQUID multiplexers. Representative noise is around 0.3 $\mu\phi_0/\sqrt{\text{Hz}}$, where $\phi_0 \equiv h/2e$ is the magnetic flux quantum, corresponding to ~1.5 p$A/\sqrt{\text{Hz}}$. The 81 pixels in each of the four BETTII detector arrays are electrically addressed with 4×22 multiplexed readouts (Fig. 11). The additional seven channels provided by the readout electronics are used for two unilluminated pixels, one always-superconducting TES sensor that will monitor pickup in the detectors, and four 'dark SQUID' channels that monitor electronic pickup in each amplifier chain. Having these extra channels permits the removal of correlated noise sources, a technique which has been shown to reduce the low-frequency $1/f$ noise knee to below 0.1 Hz (de Korte et al. 2003).

The individual column outputs are amplified by an array of SQUIDs in series that provide a gain of ≃200 to the signal. This approach has been used for decades (Welty & Martinis 1993), but the modern improvement of a low-power SQUID design and gradiometric input coils permits the amplifiers to be run in Earth's magnetic field. These SQUID series arrays are cooled to 4 K and operate in superconducting Nb shielding tubes to prevent modulation of the magnetic field as the payload rotates in the Earth frame.

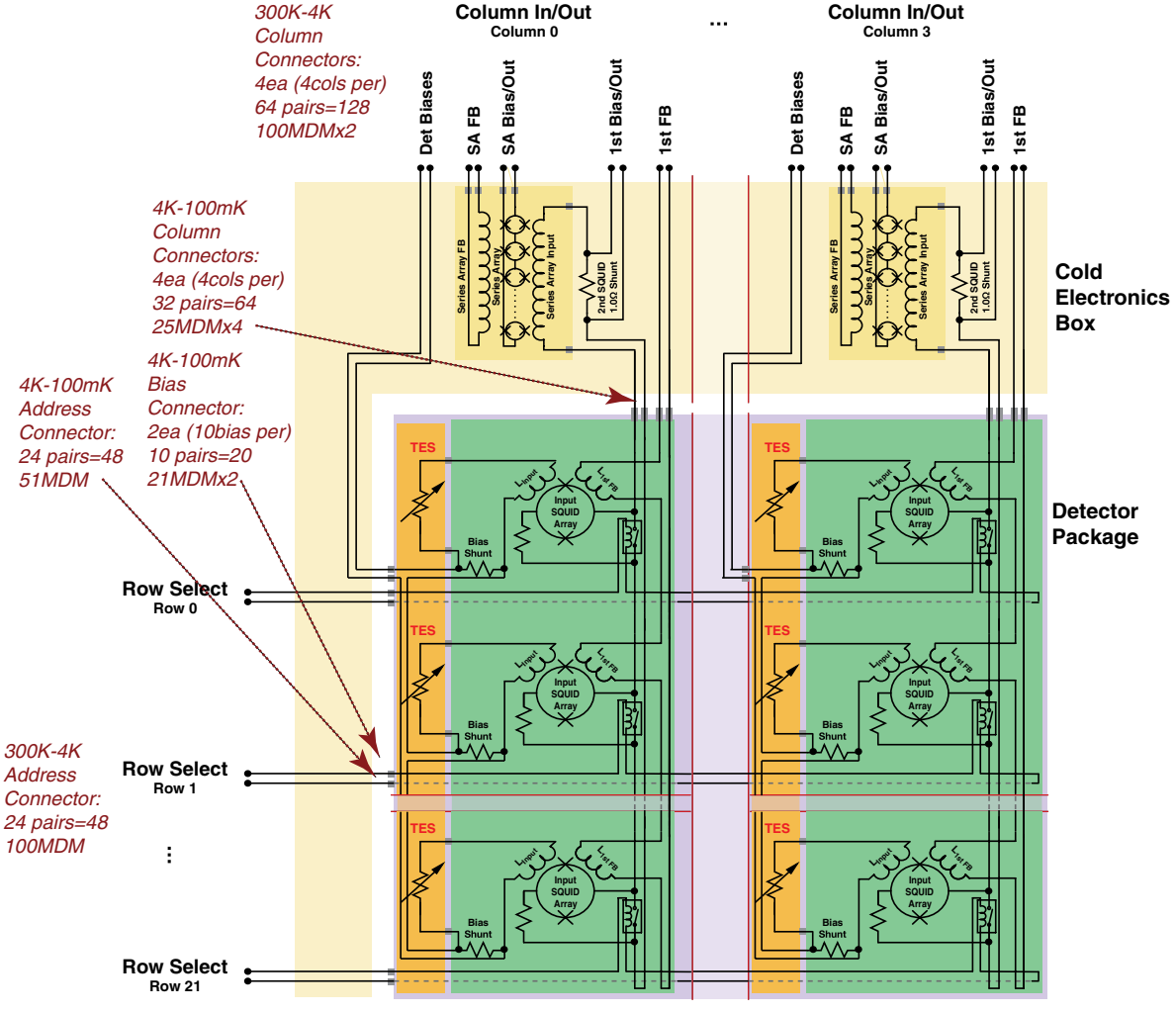

FIG. 11.—Each BETTII detector package is electrically addressed in a 4×22 multiplexed readout. This design reduces part and wire count as compared to non-multiplexed readouts, and additionally provides for diagnostic data to reduce common-mode noise sources. See the electronic edition of the *PASP* for a color version of this figure.

This content downloaded from 128.154.225.202 on Sat, 31 Jan 2015 17:02:50 PM
All use subject to JSTOR Terms and Conditions

The detectors and SQUID multiplexers operate at 300 mK. Cooling to such low temperatures is achieved by using a two-stage closed-cycle Helium-4/Helium-3 refrigerator. The refrigerator was manufactured by Chase Cryogenics, and is similar to refrigerators flown on previous balloon missions and used in GISMO (Staguhn et al. 2008).

The set of four TES and SQUID focal plane arrays is digitally controlled and read out by a single ambient-temperature Multi-Channel Electronics (MCE) unit developed by the University of British Columbia (Battistelli et al. 2008). An associated fundamental crystal clock operating at a rate of 50 MHz synchronizes the MCE data with that of other critical BETTII systems. We shift between rows after a preset number of clock cycles such that each of the 24 rows (22 addressed to the multiplexer plus two blank rows that read out only warm electronics noise) is biased on for $\sim 5.2\ \mu$s with a revisit rate of ~ 8.013 kHz. The data stream is filtered with a four-pole digital Butterworth filter at ~ 200 Hz and down-sampled to ~ 400 Hz. This provides a reasonable tradeoff between fast switching (which risks pushing against switching transients) and slow (which would increase the amount of aliased noise). As it is, the total detector system noise from all sources is predicted to be $\sim 1.5 \times 10^{-16}\ \mathrm{W}/\sqrt{(\mathrm{Hz})}$. Of this noise, 8% comes from aliased high frequency noise, which could be decreased to 4% by doubling the switching rate or increased to 17% by halving it. The MCE is connected via an optical fiber to a computer that acquires the data and that can be used to dynamically reconfigure the readout system.

2.3.2. The Tracking Channel

In addition to the FIR science channel, the BETTII instrument includes a tracking channel that operates at near-infrared wavelengths. This channel has been referred to in previous papers as the fringe tracking channel (Rizzo et al. 2012), but since the publication of that paper, the tracking channel has been redesigned and the fringe tracker component has been eliminated, leaving only the angle tracker.

The fringe tracker was designed to measure the relative phase between the two arms of the interferometer. However, it was realized that the scientific success of BETTII could be achieved without the fringe tracker. In concept, the fringe tracker would allow for correction of residual phase errors which are uncorrected by the control system. The dominant source of error, however, is the slow pendulation of the gondola. The high bandwidth of the attitude control sensors on BETTII provides confidence in the ability to reliably estimate attitude motions and "freeze" the fringes within the control system, both within the timescale of each individual scan and on the timescale of minutes. This will allow for co-adding interferograms post-flight, when a complete pointing solution is derived from all the sensor data. However, it is critical to periodically readjust the phase to avoid long-term drifts that would be caused by thermal changes. Observing calibrators, where fringes are seen in a single scan, will allow for this adjustment, and will provide valuable information on phase drift over the course of the flight. Second, by using the FIR channel for this purpose, the requirements on the optical elements within the system are greatly relaxed. In order to ensure high-quality fringes in the NIR, the quality of individual mirrors and the complexity of the mechanical design (to maintain alignment of optics, ensuring good wavefronts) must be increased. This becomes the major cost driver for the experiment. The cryostat is designed to allow for the incorporation of a fringe tracker into follow-up BETTII flights, which will help set the stage for other potential balloon interferometry experiments.

The angle tracker is designed to monitor the positions of a guide star with high accuracy, allowing BETTII to correct for differences in pointing between the two arms of the interferometer. For each arm of the interferometer, an image of the tracking star is placed on a subarray in one quadrant of an HAWAII-1RG (written in full as HgCdTe Astronomy Wide Area Infrared Imager with a $1\ \mathrm{K} \times 1\ \mathrm{K}$ resolution, Reference pixels and Guide mode, but further abbreviated to H1RG) detector array. By monitoring the centroid of these images, changes in the relative pointing of the two arms of the interferometer can be observed. This provides feedback for correcting both slow pointing drifts and for correcting fast (~ 100 Hz) motions.

Optically, the design of the angle tracker is very simple (Fig. 12). The NIR beam is transmitted by the dichroic that reflects the FIR beam. The NIR light is then relayed by a flat mirror to a single off-axis parabola camera, which creates an image on the H1RG array for each arm of the interferometer. The full array is read out during acquisition mode, while in tracking mode only the subarrays within the two quadrants that contain the tracking star images are read out to greatly improve the speed of the tracking sensor. We use a simple centroiding algorithm to measure the position of the tracking star, and convert deviations into the error signal that drives the tip/tilt mirrors in both the warm delay line and the K-mirror assembly. By monitoring the two arms separately, the angle tracker ensures that both common and noncommon pointing errors in the two arms are measured and corrected at 100 Hz.

The H1RG in the angle tracker is a 1024×1024 pixel infrared detector with complementary metal oxide semiconductor (CMOS) readout, sensitive to NIR photons from 0.6 to $5.0\ \mu$m. The H1RG multiplexer allows for the operation of the device either at low or high speeds using full frame or windowed readout. Full frame readouts are used to identify the location of the guide star images from both arms. Subsequently, two subarrays are read out in high-speed mode to track changes in the positions of the guide star images. The frame readout is about 10 ms at its highest speed (100 Hz control update rate). High-speed readout of multiple windows in an analogous configuration has been shown by Bezawada & Ives (2006), who were able to readout 32 20×20 square windows (ibid., Fig. 4) at a pixel rate of 100 kHz, in approximately 140 ms.

This content downloaded from 128.154.225.202 on Sat, 31 Jan 2015 17:02:50 PM
All use subject to JSTOR Terms and Conditions

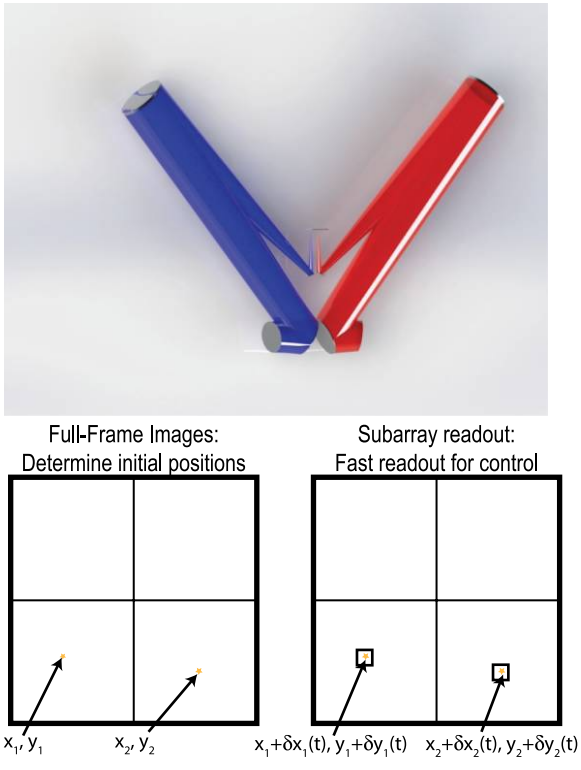

FIG. 12.—The optical design of the angle tracker consists of only three optical elements in each arm; a flat, a powered mirror, and a second flat for placing the image on the H1RG. The near-infrared image from each of the arms of the interferometer appear in different quadrants on the detector array. In full-frame mode, the initial (aligned) locations of the reference stars for each arm are determined; in tracking mode, subarrays are ready out at ~100 Hz. These images provide data on small shifts in the position of the images from the two arms, feeding into the control loop for the system. See the electronic edition of the *PASP* for a color version of this figure.

The readout is accomplished using a San Diego State University (SDSU) GENIII (Leach 1994, 1995) controller, which is ubiquitous across astronomical observatories and as such has excellent heritage and fidelity. The Leach controller is designed to be a universal CCD and CMOS readout system that requires only alteration of the Motorola digital signal processor (DSP) code, and the changing of a few connections, to operate various devices. The controller provides the power, clock level translations, video acquisition, gain adjustment, and FITS image generation. For our controller configuration, we have the standard 250 MHz timing board and IR clock driver board. However, our PC interface card is PCIe versus the standard PCI card, allowing a maximum throughput of 512 MB/s, which is required for high-speed data acquisition. Finally, we have an 8-channel IR video board for readout of the H1RG.

2.4. Exoskeleton and Control System

The final major BETTII subsystem is the exoskeleton and control system. The exoskeleton itself (shown in Fig. 1) consists of aluminum framing manufactured by 80/20 Inc., and serves as the structure for mounting flight electronics, computers, as well as the main azimuth actuator (a compensated control moment gyro, or CCMG). This structure must meet the same 10-g load requirement as the metering truss, but is not required to have the same level of stiffness. The load requirement has been verified by finite element analysis. The metering truss sits inside the exoskeleton, but the four load bearing points (at the bottom of the truss) are separated by passive vibration dampers, in order to prevent transmission of vibration from the exoskeleton to the optical system.

The three sensors critical to the control system are a star camera, three fiber optic gyroscopes (OptoLink SRS-2000), and the angle tracker. The actuators are the CCMG (azimuth), the rotation stages for the siderostats (elevation), and the tip/tilt mechanisms (fine pointing control). There is also a momentum dump mechanism.

The star camera was built in-house and is described in Benford et al. (2012). This provides 1″ RMS pointing knowledge in both R.A. and decl., and 40″ RMS knowledge of roll around the boresight. Individual frame exposures are 100 ms; astrometric computation dominates the pointing determination rate, with new pointing solutions determined every 1–2 s. However, individual frames will be acquired at the maximum readout rate, and the additional frames will be used on the ground for post-flight reconstruction of pointing. It should be noted that these results are based on ground-based observations in Greenbelt, MD, where the seeing conditions are generally unfavorable; we anticipate better results when the camera is operated in a more benign environment (such as the high altitude environment of a balloon flight). The star camera consists of a PCO.Edge camera, using a CMOS detector array, a commercial 300 mm camera lens with a mechanical focusing system, a baffle tube, and the star camera computer. The star camera is mounted on the metering truss, but the computer for reading out the camera and calculating pointing position is mounted on the exoskeleton. The star camera collects data on a $3.18 \times 2.68°$ field-of-view, and uses algorithms developed at Columbia University for the EBEX experiment (Oxley et al. 2004), modified at Cardiff University, to achieve the desired pointing accuracy. The star camera will be used in the control system to correct for gyroscope biases and drifts. It also provides "lost-in-space" pointing determination capability.

BETTII uses three single-axis fiber optic gyroscopes mounted orthogonally. The gyroscopes provide fast readout (400 Hz, with bandwidth of ~50 Hz) and specifications for drift and noise are 0.005 arcsecond/second and $0.0005\ \mathrm{deg}/\sqrt{\mathrm{hr}}$, respectively. The gyroscopes serve as the high-speed sensor for gondola motion. By combining these data with results from the star camera, it will be possible to control the gondola pointing to within a few arcseconds in order to acquire a guide star on the angle tracker. In the laboratory, this level of pointing stability has already been achieved. It should be noted, however, that pendulum motion representative of flight conditions is difficult to reproduce, and

This content downloaded from 128.154.225.202 on Sat, 31 Jan 2015 17:02:50 PM
All use subject to JSTOR Terms and Conditions

therefore these results are not necessarily representative of on-flight performance. A more detailed discussion of these results, and the overall function of the BETTII control system, is presented by Rizzo et al. (2014a).

When the guide star is in the angle sensor's field-of-view (within about 10" of field center), the angle tracker uses it to determine position via a simple centroiding algorithm. The deviation from the desired star location on the detector, corresponding to perfect optical alignment of both arms, is then fed into the tip/tilt mechanisms.

Azimuth control of the gondola is provided by the compensated control moment gyro (CCMG; Fig. 13). The two wheels in the CCMG spin at a constant rate of 3051.8 RPM (synchronized with the readout from the TES detector arrays), providing 10.4 Nms of angular momentum. These are mounted on a gimbal which changes the orientation of the wheels. In the null-torque position, the two wheels are oriented back-to-back. By changing the orientation of the wheels by equal and opposite amounts on the gimbal, they combine to provide a torque that rotates the gondola. The constant speed operation of the wheels provides two major advantages: it minimizes power usage, and it results in a time-constant vibration profile, allowing for effective mitigation. Control of the pointing elevation is provided by rotating the siderostats using rotation stages. Effectively, the pointing methodology for the interferometer is equivalent to an altitude/azimuth telescope. The CCMG has been fully tested under similar conditions as expected during flight (i.e., both cold and at low pressure), and meets all requirements for the BETTII control system.

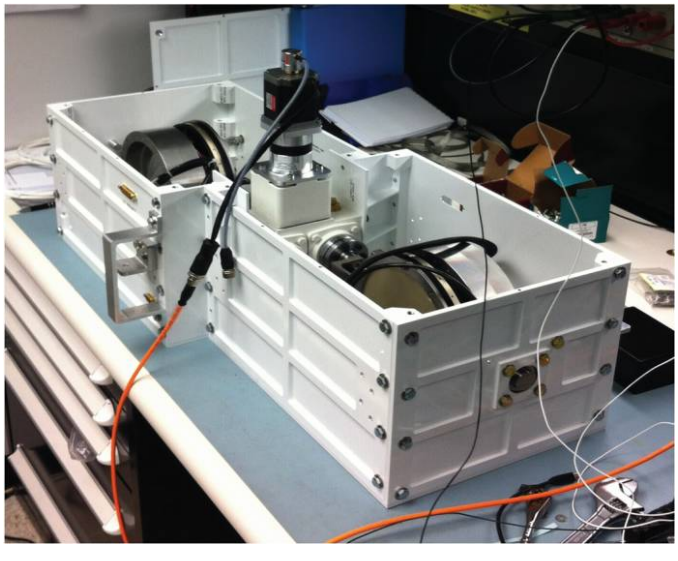

FIG. 13.—The completed CCMG is shown here; the picture was taken with the top cover removed during testing of the assembly. The two reaction wheels are clearly visible. A motor located in the center of the assembly is used to pivot the wheels in equal and opposite directions around the long axis of the assembly. See the electronic edition of the *PASP* for a color version of this figure.

TABLE 3
POINTING CONTROL MODES

Mode	Sensors Used	Purpose
Lost	Star Camera	Determine Pointing
Slew	Gyros	Large pointing changes
Acquire	Camera & Gyro	Lock gondola pointing
Tracking	Angle tracker	Lock instrument pointing

The pointing control system has four modes of operation, as detailed in Table 3. Two of these (tracking mode and slew mode) are diagrammed in Figure 14. Lost mode simply uses the star camera to determine gondola pointing. In slew mode, where no guide star appears on the angle tracker yet, we use the star camera and the gyroscopes to generate the attitude errors. This is a common pointing configuration, used on other balloons as well as on spacecraft, where the star camera information is used to estimate and correct for the gyroscope bias drift. Once the gondola is correctly pointed, the system switches to acquire mode, where the gondola pointing is locked through readouts from both the star camera and the gyros. While locked, the image of the guide star is located on the H1RG array, and subarray readout is configured for tracking mode. With the guide star acquired and locked by the angle sensor, the control signal changes. The deflection of both tip/tilt mirrors required to keep

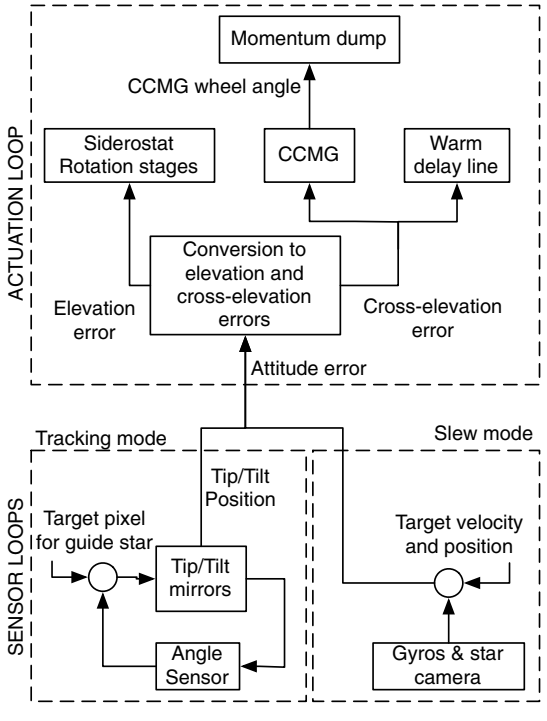

FIG. 14.—The tracking and slew modes of the BETTII control system are shown schematically here. The actuation for these two modes is nearly identical, as are the control loop algorithms; the primary difference is in the sensors used to provide feedback.

This content downloaded from 128.154.225.202 on Sat, 31 Jan 2015 17:02:50 PM
All use subject to JSTOR Terms and Conditions

the guide star locked in both arms is now the best estimate of BETTII's attitude. Both the control signal and the physical motions of the tip/tilt mirrors, as measured with encoders on the tip/tilts, are recorded. Since this measurement is tied to the optical system, it does not drift over time. Combining the tip/tilt position, the gyros, and the star camera can be used in post-processing to build a robust estimator that can estimate the attitude to 0.1″ rms over a few minutes. This is investigated in detail by Rizzo et al. (2014a).

BETTII also has an optical path difference control loop, with the purpose of freezing the fringes as the payload is pendulating. On short timescales, the phase noise is almost exclusively caused by attitude errors. Hence, measuring the attitude errors provides a good estimator of the phase errors. These phase errors are fed to a fast linear actuator, the "warm delay line", which compensates for varying external optical path length between the source and the siderostats. This has the effect of freezing the phase before light enters the cryogenic section of BETTII, where double-Fourier interferometry can happen. The warm delay line was discussed previously in this paper (see section 2.2). It is important to remember that, for BETTII, pointing knowledge is more important than the actual pointing of the gondola. Since pointing differences result in path differences between the two arms of the interferometer (1" of pointing change results in ∼40 μm of phase change), knowledge of small pointing changes is necessary to accurately remove these phase changes using the warm delay line.

Finally, BETTII includes a momentum dump mechanism which can rotate the flight train with respect to the gondola, effectively dumping momentum through the balloon ladder into the balloon. As the CCMG is used to slew the gondola, the momentum dump mechanism will be activated through a simple PID loop. This will prevent the possible build-up of angular momentum in the gondola. This dump mechanism is based upon designs which have flown previously (Fixsen et al. 1996).

Additional sensors attached to the exoskeleton will provide ancillary housekeeping data. These include a sun sensor, accelerometers, magnetometers, and inclinometers. In addition to the general housekeeping purposes, these sensors will be used for post-flight assessment of the payload's performance and for data quality determination (e.g., magnetometer data can be used to monitor magnetic field conditions which can impact detector readout). None of these sensors are integral to the control system or to the acquisition of science data. Other such housekeeping systems include thermometry (∼60 thermometers will be located at various positions on the gondola, with additional thermometers inside the cryostat) and laser/quad cell systems for measuring sag and vibration of the gondola.

3. PREDICTED PERFORMANCE

Following the BETTII flight, the team will conduct a detailed analysis of the system performance. This will include analysis of the science data and characterization of scientific performance, and will also include detailed analysis of all housekeeping data to understand the behavior of the system, include mechanical and thermal behavior, control system operation, and cryostat behavior. Performance predictions for all of the subsystems can be made based upon ongoing laboratory testing, and such tests will be discussed in future publications. It is also possible to predict the overall scientific performance.

The overall scientific performance of BETTII will be limited by the combination of amplitude noise and phase noise. Amplitude noise sources, such as photon noise from the interferometric source, detector noise, sky noise, and background photons from the warm optics, lead to uncertainty in the measured amplitude of the interferometric fringes. Phase noise sources, on the other hand, can lead to both a "blurring" of fringes reducing the overall signal in the interferometric fringes, and can distort the fringe pattern itself, leading to incorrect spectral reconstruction.

For BETTII, amplitude noise arises from thermal emission from optical elements, from the sky, from inherent noise of the detector arrays, and from the source itself. Of these, the thermal emission from optical elements dominates (Table 4). The Noise Equivalent Power (NEP) of the detectors is 3.00×10^{-16} W$/\sqrt{\text{Hz}}$ in the short band, and 3.00×10^{-16} W$/\sqrt{\text{Hz}}$ in the long band. This combined with the background power leads to a total instrument NEP of 1.38×10^{-15} W$/\sqrt{\text{Hz}}$ in the short-wavelength band, and 0.74×10^{-15} W$/\sqrt{\text{Hz}}$ in the long-wavelength band.

In the absence of phase noise, the Minimum Detectable Flux Density (MDFD) in the interferogram domain is of 3.0 Jy in the short wavelength band and 4.2 Jy in the long wavelength band, assuming 200 3-s scans are coadded (10 minutes of total integration time on source). Sensitivity is reduced in the presence of phase noise. BETTII's control system will allow overall pointing of the system to better than 10", corresponding to ∼400 μm of phase difference. Further, the control system sensors should allow estimation of residual phase noise with an accuracy of ∼4 μm (RMS), so that we can use the delay lines

TABLE 4

PREDICTED PERFORMANCE

Parameter	Band 1 (30–50 μm)	Band 2 (60–90 μm)
Photon power from the sky	35 pW	36 pW
Photon power from the window	40 pW	18 pW
Photon power from the optics	108 pW	38 pW
Total NEP	$1.41 \times 10^{-15} W/\sqrt{\text{Hz}}$	$0.78 \times 10^{-15} W/\sqrt{\text{Hz}}$

This content downloaded from 128.154.225.202 on Sat, 31 Jan 2015 17:02:50 PM
All use subject to JSTOR Terms and Conditions

to correct most of the leftover phase difference; this increases the MDFD for BETTII to 4.3 Jy in the short-wavelength FIR band, and 4.7 Jy in the long-wavelength FIR band. These correspond to a conservative estimate of point source sensitivity, assuming 10 minutes integration and a spectral resolution of $R = 10$, of 34 Jy and 32 Jy for the short and long bands, respectively. A much more complete discussion of the expected performance and of the impact of phase noise on sensitivity can be found in (Rizzo et al. 2014b).

For the first BETTII flight, Ceres will serve as a calibration source; with a flux of ~800 Jy in the 30–60 μm band, a S/N of ~20 should be achieved in a single interferogram scan. Other bright solar system asteroids could also serve this purpose. For star formation targets of interest to BETTII, exact fluxes are not generally known. Typically, these objects saturate the detectors in WISE 22 μm data, implying fluxes >12 Jy. Since the spectral energy distribution of these objects is also rising towards long wavelengths, the fluxes in the BETTII bands are likely somewhat higher than 12 Jy. This results in single-track spectral S/N of ~2.5 for a 10-minute observation. For the first flight, as the focus is on proving the instrument and ensuring high-quality data, it is likely that only 1–2 fields will be observed; each field will contain a few (2–5) unique sources.

While the BETTII payload is designed to minimize sources of systematic noise, it is not possible to completely eliminate such sources. Ongoing testing of the BETTII subsystems, and future testing of the full BETTII system in the laboratory, will be used to identify potential sources of systematic errors, to find mitigation methods for them, and to develop data analysis techniques for addressing them (Fixsen et al. 1996). Further, housekeeping sensors on BETTII (e.g., accelerometers, thermometers) should allow better assessment of potential sources of systematic errors while on float, potentially allowing improved post-flight analysis, and leading to design improvements for successors to BETTII. A full assessment of the sources of systematic noise in the system will be performed following the first BETTII flight.

4. POTENTIAL SCIENCE PROGRAMS

BETTII, when operational, will provide a unique ability to conduct spatially-resolved spectroscopy. Because BETTII has a single fixed baseline, relying on sky rotation to provide an arc in the $u - v$ domain, reconstruction of complex images would be extremely difficult or impossible. However, even with the limited baseline coverage, BETTII will be able to isolate the flux from individual point sources within its field-of-view and obtain FIR spectra of each of these sources. This will allow us to disentangle the spectra of multiple sources which have been previously unresolved at these long wavelengths.

BETTII's first flight, planned for 2015 fall, will focus on observations of clustered star forming regions. These regions have a high density of young stellar objects, and are sufficiently distant that individual sources are unresolved by existing FIR facilities. With spatially-resolved spectroscopy, it will be possible to determine the spectral energy distribution of individual YSOs, while also searching for broad spectral features due to the presence of water ice or minerals.

BETTII can also be used to isolate sources of emission from Active Galactic Nuclei (Spinoglio et al. 2005). For instance, in the case of NGC 1068, radio CO maps have shown two distinct sources of emission near the core of the galaxy. These sources, with an angular separation of only a few arcseconds, are unresolved by *Spitzer* and *Herschel*, but BETTII will resolve their individual spectra. Further, the ability of BETTII to determine the distances between point symmetric objects will allow measurement of the distance between the unresolved nucleus and the surrounding disks of AGN.

BETTII may also be able to address other scientific topics as well. A more complete discussion of the scientific cases mentioned above can be found in Rinehart (2010).

5. DISCUSSION AND IMPLICATIONS

BETTII is currently on schedule for first launch in 2015 fall from Fort Sumner, New Mexico. The scientific focus of this flight will be studies of clustered star formation. In addition, repeated observations will be made of calibration sources (e.g., infrared-bright stars), in order to fully characterize the instrument, the gondola structure, and the control system. Based upon experience garnered from this first flight, we anticipate that BETTII will have additional future flights to explore a sample of star forming clusters and active galactic nuclei. We also plan to use the knowledge gained from the first flight to design and incorporate improvements that will enhance the overall performance of the system.

The two major limitations of the BETTII experiment are the sensitivity and the sparse coverage of the synthetic aperture (in interferometric terms, the $u - v$ plane). Potential avenues for improving the overall sensitivity of BETTII include increasing the size of individual collecting apertures and potentially cooling the optics. Potential avenues for improving the coverage of the synthetic aperture include the inclusion of additional baselines and/or making the siderostat mirrors movable along the length of the truss. The former would provide additional arcs in the $u - v$ plane, while the latter would allow for radial coverage of the $u - v$ plane.

In the long-term, space-based interferometers will be needed to address some of the most ambitious scientific questions posed by the astronomical community, covering a wide range of scientific questions and a wide range of wavelengths (Rinehart et al., in preparation). BETTII will provide a system-level demonstration of an interferometer operating in a space-like environment, and as such becomes a stepping stone to future space interferometers.

The material presented in this paper is based upon work supported by NASA Science Mission Directorate through the ROSES/APRA program, with additional support provided by

This content downloaded from 128.154.225.202 on Sat, 31 Jan 2015 17:02:50 PM
All use subject to JSTOR Terms and Conditions

NASA's Goddard Space Flight Center. Work by T. Veach was supported by an appointment to the NASA Postdoctoral Program at GSFC, administered by the Oak Ridge Associated Universities under contract with NASA. Contributions to this project were also made by a large number of undergraduate students, including: S. Gomillion, J. Doiron, S. Gore, B. Hoffman, W. Tierney, R. Curley, T. Kale, T. Handleton, S. Shapoval, M. Canaparro, D. Andrade, J. Stokes, C. Gibbons, S. Weinreich, J. Alcorn, A. Rau, S. Padder, P. Nehme, L. Oliviera, H. Spooner, C. Wagner, A. Cotto, N. Mihalko, Y. Okafor, P. Taraschi, J. Gibson, and Y. Huertes-Morales. The BETTII program at Cardiff University and UCL is supported by an STFC PRD grant.

REFERENCES

Acke, B., Min, M., Dominik, C., Vandenbussche, B., Sibthorpe, B., Waelkens, C., Olofsson, G., Degroote, P., et al. 2012, A&A, 540, A 125

Allen, C. A., Abrahams, J., Benford, D. J., Chervenak, J. A., Chuss, D. T., Staguhn, J. G., Miller, T. M., Moseley, S. H., et al. 2006, in Astronomical Telescopes and Instrumentation ed.J. Zmuidzinas, W. S. Holland, S. Withington, & W. D. Duncan (Bellingham: SPIE), 62750B–62750B–8

Battistelli, E. S., Amiri, M., Burger, B., Halpern, M., Knotek, S., Ellis, M., Gao, X., Kelly, D., et al. 2008, J. Low Temp. Phys., 151, 908

Benford, D. J., Fixsen, D. J., Rinehart, S. A., Rizzo, M., Maher, S. F., & Barry, R. K. 2012, in Astronomical Telescopes and Instrumentation, 84442P–84442P–11

Benford, D. F., Jhabvala, C., Staguhn, J., Sharp, E., Wollack, E., Fixsen, D., & Rinehart, S. 2014, in Astronomical Telescopes and Instrumentation, ed. W. S. Holland, & J. Zmuidzinas (Bellingham: SPIE)

Benford, D. J., Staguhn, J. G., Allen, C. A., & Sharp, E. H. 2008, in Astronomical Telescopes and Instrumentation, ed. W. D. Duncan, W. S. Holland, S. Withington, & J. Zmuidzinas (Bellingham: SPIE), 702026–702026–10

Bezawada, N., & Ives, D. 2006, in Astronomical Telescopes and Instrumentation, ed. D. A. Dorn, & A. D. Holland (Bellingham: SPIE), 62760O–62760O–12

Chuss, D. T., Wollack, E. J., Henry, R., Hui, H., Juarez, A. J., Krejny, M., Moseley, S. H., & Novak, G. 2012, Appl. Opt., 51, 197

Chuss, D. T., Wollack, E. J., Moseley, S. H., & Novak, G. 2006, Appl. Opt., 45, 5107

de Korte, P. A. J., Beyer, J., Deiker, S., Hilton, G. C., Irwin, K. D., MacIntosh, M., Nam, S. W., Reintsema, C. D., et al. 2003, Rev. Sci. Instrum., 74, 3807

Fixsen, D. J., Cheng, E. S., Cottingham, D. A., Folz, W. C., Inman, C. A., Kowitt, M. S., Meyer, S. S., Page, L. A., et al. 1996, ApJ, 470, 63

Harwit, M., Leisawitz, D., & Rinehart, S. 2006, NewA Rev., 50, 228

Kamp, I., Thi, W. F., Meeus, G., Woitke, P., Pinte, C., Meijerink, R., Spaans, M., Pascucci, I., et al. 2013, A&A, 559, A 24

Leach, R. W. 1994, Optical Astronomy from the Earth and Moon, 55, 113

———. 1995, New Developments in Array Technology and Applications, 167, 49

Leisawitz, D., Baker, C., Barger, A., Benford, D., Blain, A., Boyle, R., Broderick, R., Budinoff, J., et al. 2007, Adv. Space Res., 40, 689

Leisawitz, D., Bolcar, M. R., Lyon, R. G., Maher, S. F., Memarsadeghi, N., Rinehart, S. A., & Sinukoff, E. J. 2012, in Astronomical Telescopes and Instrumentation, ed. F. Delplancke, J. K. Rajagopal, & F. Malbet (Bellingham: SPIE), 84450A–84450A–10

Mariotti, J. M., & Ridgway, S. T. 1988, A&A, 195, 350

Nguyen, H. T., Schulz, B., Levenson, L., Amblard, A., Arumugam, V., Aussel, H., Babbedge, T., Blain, A., et al. 2010, A&A, 518, L 5

Ogasaka, Y., Tueller, J., Yamashita, K., Serlemitsos, P., Shibata, R., Tamura, K., Furuzawa, A., Miyazawa, T., et al. 2005, in Optics & Photonics, ed. O. Citterio, & S. L. O'Dell (Bellingham: SPIE), 59000R–59000R–8

Oxley, P., Ade, P. A., Baccigalupi, C., deBernardis, P., Cho, H.-M., Devlin, M. J., Hanany, S., Johnson, B. R., et al. 2004, in Astronomical Telescopes and Instrumentation, ed. M. Strojnik (Bellingham: SPIE), 320–331

Rigby, E. E., Maddox, S. J., Dunne, L., Negrello, M., Smith, D. J. B., González-Nuevo, J., Herranz, D., López-Caniego, M., et al. 2011, MNRAS, 415, 2336

Rinehart, S. 2010, in Astronomical Telescopes and Instrumentation (Bellingham: SPIE), 7734, 77340 K

Rinehart, S. A., Barclay, R. B., Barry, R. K., Benford, D. J., Calhoun, P. C., Fixsen, D. J., Gorman, E. T., Jackson, M. L., et al. 2012, in SPIE Astronomical Telescopes and Instrumentation (Bellingham: SPIE), 844508–844508–15

Rinehart, S. A., Rizzo, M., Fixsen, D., Ade, P., Barclay, R., Barry, R., Benford, D., Dhabal, A., et al. 2014, in Astronomical Telescopes and Instrumentation, ed. J. K. Rajagopal, M. J. Creech-Eakman, & F. Malbet (Bellingham: SPIE)

Rizzo, M., Rinehart, S. A., J, B. D., Fixsen, D., & Silverberg, R. 2014a , in Astronomical Telescopes and Instrumentation, ed. J. M. J. Oschmann, M. Clampin, G. G. Fazio, & H. A. MacEwen (Bellingham: SPIE)

Rizzo, M. J., Dhabal, A., Mundy, L., Fixsen, D. J., Rinehart, S. A., Benford, D. F., Leisawitz, D. T., & Silverberg, R. 2014b, ApJ, in press

Rizzo, M. J., Rinehart, S. A., Barry, R. K., Benford, D. J., Fixsen, D. J., Kale, T., Leisawitz, D. T., Lyon, R. G., et al. 2012, in Astronomical Telescopes and Instrumentation, ed. F. Delplancke, J. K. Rajagopal, & F. Malbet (Bellingham: SPIE), 84451 T

Spinoglio, L., Malkan, M. A., Smith, H. A., & Gonzalez Alfonso, E., Fischer, J. 2005, ApJ, 623, 123

Staguhn, J., Allen, C., Benford, D., Sharp, E., Ames, T., Arendt, R., Chuss, D., Dwek, E., et al. 2008, J. Low Temp. Phys., 151, 709

Staguhn, J. G., Benford, D. J., Allen, C. A., Moseley, S. H., Sharp, E. H., Ames, T. J., Brunswig, W., Chuss, D. T., et al. 2006, in Astronomical Telescopes and Instrumentation, ed. J. Zmuidzinas, W. S. Holland, S. Withington, & W. D. Duncan (Bellingham: SPIE), 62751D–62751D–9

Staguhn, J. G., Kovćs, A., Arendt, R. G., Benford, D. J., Decarli, R., Dweak, E., Fixsen, D. J., Hilton, G. C., et al. 2014, ApJ, in press

Veach, T., Rinehart, S., Mentzell, J. E., Fixsen, D., Rizzo, M., Gibbons, C., & Benford, D. 2014, in Astronomical Telescopes and Instrumentation, ed. J. K. Rajagopal, M. J. Creech-Eakman, & F. Malbet (Bellingham: SPIE)

Welty, R. P., & Martinis, J. M. 1993, IEEE Transactions on Applied Superconductivity, 3, 2605

This content downloaded from 128.154.225.202 on Sat, 31 Jan 2015 17:02:50 PM
All use subject to JSTOR Terms and Conditions